Experimental Verification of Modal Characteristics of Vehicle Computing Model

J. Melcer [1,a]

[1] *University of Žilina, Faculty of Civil Engineering, Slovak Republic*
[a] *jozef.melcer@fstav.uniza.sk*

Abstract: For the numerical simulation of vehicle motion along transport structures various computing models of vehicles were created. To obtaine relevant results of numerical simulation the properties of computing model must correspond to the reality. The parameters of vehicle computing model were tuned on the basis of in situ experimental test. The modal characteristics of computing model were compared with modal characteristics of real vehicle.

Keywords: experiment; numerical simulation; vehicle; computing model; modal characteristics.

1 Introduction

Solution of the problem of vehicle – road or vehicle – bridge interaction demands to create computing model of vehicle and computing model of a structure. The computing model of vehicle can be created on various levels – one two or three dimensional. For the modeling of moving load effect on pavements the three dimensional computing model of vehicle Tatra 815 was created. The properties of the model were verified by experimental test carried out on actual vehicle. The modal characteristic of computing model and modal characteristics of actual vehicle were mutually compared.

2 Vehicle computing model

The space multi-body computing model of vehicle Tatra 815 was created, Fig. 1, [1]. The model has 9 mass degrees of freedom.

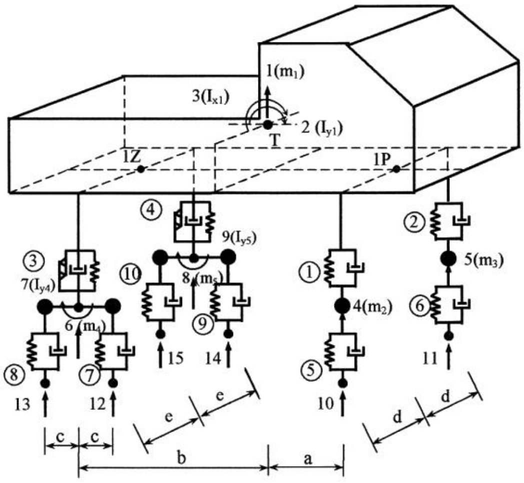

Fig. 1: Space computing model of vehicle Tatra 815.

The mass characteristics and stiffness characteristics were verify on the real vehicle. The vehicle was weighted as a whole and every axle individually. The results are put into Tab. 1.

Tab. 1: Mass of full and empty vehicle.

	m_C [kg]	m_{LF} [kg]	m_{RF} [kg]	m_{LR} [kg]	m_{RR} [kg]
full vehicle	23 250	2 840	2 830	8 905	8 675
empty vehicle	11 990	2 300	2 300	3 695	3 695
mass difference	11 260	540	530	5 210	4 980

For the determination of stiffness constants of vehicle computing model the distances of characteristic points of vehicle bed from comparative plane for empty and full vehicle were measured. The distances were measured by laser distance meter Leica DISTO^{TM} A5. Tire pressing were evaluated from digital snaps. The marking of vehicle bed characteristic points and vehicle wheels are in the Fig. 2.

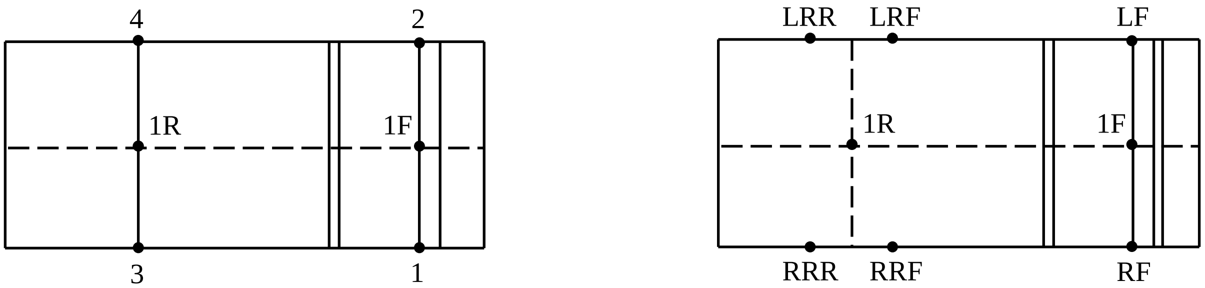

Fig. 2: Marking of vehicle characteristics points.

The distances of vehicle bed characteristic points in regard of comparative plane are put into Tab. 2 and tire pressing into Tab. 3.

Tab. 2: Distances of vehicle bed characteristic points in regard of comparative plane.

	w_1 [mm]	w_2 [mm]	w_3 [mm]	w_4 [mm]
full vehicle	1 410	1 392	1 507	1 507
empty vehicle	1 364	1 345	1 447	1 441
distance difference	46	47	63	66

Tab. 3: Tire pressing of individual wheels.

	w_{RF} [mm]	w_{LF} [mm]	w_{RRF} [mm]	w_{RRR} [mm]	w_{LRF} [mm]	w_{LRR} [mm]
tire pressing	3.2	3.4	9.7	9.8	10.2	10.3

The forces activated the displacements of vehicle bed characteristic points are put into Tab. 4 and forces activated the tire displacements of individual wheels are put into Tab. 5.

Tab. 4: Forces activated the displacements of vehicle bed characteristic points.

	F_1 [N]	F_2 [N]	F_3 [N]	F_4 [N]
force	5 300	5 400	49 800	52 100

Tab. 5: Forces activated the tire displacements of individual wheels.

	F_{RF} [N]	F_{LF} [N]	F_{RRF} [N]	F_{RRR} k_7 =	F_{LRF} [N]	F_{LRR} [N]
force	5 300	5 400	24 900	24 900	26 050	26 050

From the forces put into Tab. 4 and 5 and from displacements put into Tab. 2 and 3 the stiffness constants of individual connecting members of vehicle computing model were calculated. The stiffness constants were calculated in two variants. In variant 1 the stiffness constants were calculated from average forces and average displacements, Tab. 6. It means that the values for left and right side of vehicle are the same. In variant 2 the stiffness constants were calculated for actual values, Tab. 7.

Tab. 6: Stiffness constants for variant 1 – average values.

	$k_1 = k_2$ [N/m]	$k_3 = k_4$ [N/m]	$k_5 = k_6$ [N/m]	$k_7 = k_8 = k_9 = k_{10}$ [N/m]
stiffness constants	123 843	934 862	1 621 212	2 547 500

Tab. 7: Stiffness constants for variant 2 – actual values.

	k_1 [N/m]	k_2 [N/m]	k_3 [N/m]	k_4 [N/m]	k_5 [N/m]
stiffness constants	123 831	123 854	935 207	934 525	1 656 256
	k_6 [N/m]	k_7 [N/m]	k_8 [N/m]	k_9 [N/m]	k_{10} [N/m]
stiffness constants	1 588 235	2 567 010	2 540 816	2 553 922	2 529 126

For the variant 1 and 2 the natural frequencies and natural model were calculated.
Results for variant 1:

Diagonal mass matrix

$$\mathbf{\{m\}_D} = \{m_1, I_{y1}, I_{x1}, m_2, m_3, m_4, I_{y4}, m_5, I_{y5}\}_D =$$
$$= \{20200, 54822, 20196, 455, 455, 1070, 466, 1070, 466\}_D \quad [\text{kg, kg.m}^2].$$

Diagonal matrix of stiffness constants

$$\mathbf{\{k_i\}_D} = \{k_1, k_2, k_3, k_4, k_5, k_6, k_7, k_8, k_9, k_{10}\}_D =$$
$$= \{123843, 123843, 934862, 934862, 1621212, 1621212, 2547500, 2547500, 2547500, 2547500\}_D \quad [\text{N/m}].$$

Natural frequencies

$$\mathbf{\{f\}} = \{f_{(1)}, f_{(2)}, f_{(3)}, f_{(4)}, f_{(5)}, f_{(6)}, f_{(7)}, f_{(8)}, f_{(9)}\} =$$
$$= \{1.14, \ 1.46, \ 1.68, \ 9.86, \ 9.86, \ 10.98, \ 10.98, \ 11.96, \ 11.96\} \quad [\text{Hz}].$$

Natural modes – modal matrix

$$\mathbf{[r[} = \left\lfloor \{r_{(1)}\} \ \{r_{(2)}\} \ \{r_{(3)}\} \ \{r_{(4)}\} \ \{r_{(5)}\} \ \{r_{(6)}\} \ \{r_{(7)}\} \ \{r_{(8)}\} \ \{r_{(9)}\} \right\rfloor =$$

$$= \begin{bmatrix} -0.7589 & 0.0000 & -0.8644 & 0.0000 & 0.0022 & 0.0000 & 0.0000 & 0.0000 & -0.0118 \\ 0.5935 & 0.0000 & -0.4074 & 0.0000 & -0.0026 & 0.0000 & 0.0000 & 0.0000 & -0.0047 \\ 0.0000 & 0.9725 & 0.0000 & -0.0022 & 0.0000 & 0.0000 & 0.0000 & -0.0114 & 0.0000 \\ -0.1884 & -0.0701 & 0.0301 & -0.7071 & -0.7071 & 0.0000 & 0.0000 & -0.0017 & -0.0004 \\ -0.1884 & 0.0701 & 0.0301 & 0.7071 & -0.7071 & 0.0000 & 0.0000 & 0.0017 & -0.0004 \\ -0.0189 & -0.1489 & -0.2060 & 0.0011 & -0.0002 & 0.0000 & 0.0000 & -0.7071 & 0.7071 \\ 0.0000 & 0.0000 & 0.0000 & 0.0000 & 0.0000 & 1.0000 & 0.0000 & 0.0000 & 0.0000 \\ -0.0189 & 0.1489 & -0.2060 & -0.0011 & -0.0002 & 0.0000 & 0.0000 & 0.7071 & 0.7071 \\ 0.0000 & 0.0000 & 0.0000 & 0.0000 & 0.0000 & 0.0000 & 1.0000 & 0.0000 & 0.0000 \end{bmatrix}$$

Results for variant 2:

Diagonal mass matrix

$$\mathbf{\{m\}_D} = \{m_1, I_{y1}, I_{x1}, m_2, m_3, m_4, I_{y4}, m_5, I_{y5}\}_D =$$
$$= \{20200, 54822, 20196, 455, 455, 1070, 466, 1070, 466\}_D \quad [\text{kg, kg.m}^2].$$

Diagonal matrix of stiffness constants

$$\mathbf{\{k_i\}_D} = \{k_1, k_2, k_3, k_4, k_5, k_6, k_7, k_8, k_9, k_{10}\}_D =$$
$$= \{123831, 123854, 935207, 934525, 1656250, 1588235, 2567010, 2540816, 2553922, 2529126\}_D \quad [\text{N/m}].$$

Natural frequencies

$$\mathbf{\{f\}} = \{f_{(1)}, f_{(2)}, f_{(3)}, f_{(4)}, f_{(5)}, f_{(6)}, f_{(7)}, f_{(8)}, f_{(9)}\} =$$
$$= \{1.14, \ 1.46, \ 1.68, \ 9.76, \ 9.95, \ 10.96, \ 10.99, \ 11.95, \ 11.98\} \quad [\text{Hz}]$$

Natural modes – modal matrix

$$\mathbf{[r[} = \lfloor \{r_{(1)}\} \quad \{r_{(2)}\} \quad \{r_{(3)}\} \quad \{r_{(4)}\} \quad \{r_{(5)}\} \quad \{r_{(6)}\} \quad \{r_{(7)}\} \quad \{r_{(8)}\} \quad \{r_{(9)}\} \rfloor =$$

$$\begin{bmatrix} 0.7589 & -0.0008 & -0.8644 & -0.0016 & 0.0016 & -0.0001 & 0.0001 & -0.0070 & -0.0094 \\ -0.5935 & -0.0013 & -0.4074 & 0.0018 & -0.0018 & 0.0000 & 0.0000 & -0.0028 & -0.0037 \\ 0.0014 & -0.9725 & 0.0023 & -0.0016 & -0.0015 & -0.0001 & -0.0001 & -0.0092 & 0.0068 \\ 0.1845 & 0.0689 & 0.0293 & -0.0109 & -0.9999 & 0.0000 & 0.0000 & -0.0017 & 0.0006 \\ 0.1922 & -0.0712 & 0.0309 & 0.9999 & -0.0105 & 0.0000 & 0.0000 & 0.0010 & -0.0013 \\ 0.0186 & 0.1483 & -0.2059 & 0.0009 & 0.0005 & 0.0000 & -0.0180 & -0.1438 & 0.9887 \\ 0.0001 & 0.0011 & -0.0016 & 0.0000 & 0.0000 & -0.0001 & -0.9998 & 0.0061 & -0.0411 \\ 0.0191 & -0.1495 & -0.2060 & -0.0005 & 0.0009 & 0.0171 & 0.0000 & 0.9887 & 0.1432 \\ 0.0001 & -0.0011 & -0.0015 & 0.0000 & 0.0000 & 0.9998 & -0.0001 & -0.0390 & -0.0055 \end{bmatrix}$$

3 Experimental test

To verify the modal characteristics of vehicle computing model the in situ experimental test on vehicle was carried out. The purpose of the test was to excite vibration very closed to natural vibration. Twelve test trip of vehicle were realized during the experiment. The list of individual runs within the test is put into the Tab. 8.

Tab. 8: List of individual runs within the test.

No. of run	description of run
1	run over standard obstacle
2	run over standard obstacle
3	run over plank of dimensions 50×320 mm
4	run over plank of dimensions 50×320 mm
5	run by right wheel over plank in longitudinal direction (length 3.5 m)
6	run by right wheel over plank in longitudinal direction (length 3.5 m)
7	run by right wheel over standard obstacle and by left wheel over plank (obstacles are shift 0.9 m in longitudinal direction)
8	run by right wheel over standard obstacle and by left wheel over plank (obstacles are shift 1.2 m in longitudinal direction)
9	run to left-handed arch
10	run to left-handed arch
11	run to left-handed arch plus normal obstacle in the left track
12	run by right wheel along street curb and by left wheel along pavement

The vehicle response was registered by four accelerometers Bjuer-Kjaer BK 4508. Sensor BK1 was located on the front axle, BK2 on the rear axle of vehicle in vertical direction. Sensor BK3 was located on the bed of vehicle in horizontal direction and sensor BK4 in the front the frame of vehicle body in vertical direction. The signal was amplified, digitized by A/D interface and stored in computer. The spectral analysis of individual records was carried out. Power spectral densities (PSD) were used for evaluation of natural frequencies. The values of dominant frequencies obtained from frequency spectra calculated from individual records are put into Tab. 9. The values of numerically and experimentally obtained natural frequencies are mutually compared in the Tab. 10. The results introduced in Tab. 9 and 10 are supported by figures of power spectral densities shown in Fig. 3, 4, 5.

Tab. 9: Dominant frequencies correspond to individual sensors and individual runs.

No. of run	sensor BK1	sensor BK2	sensor BK3	sensor BK4
1	10.00	2.66	1.20;12.14	1.21
2	1.20; 9.99; 10.97; 12.18	2.92	1.45; 12.14	1.19
3	1.44; 9.99; 10.47	2.65	1.20; 1.67	1.46; 2.91
4	1.67	2.89	1.46	1.69
5	9.73; 10.97	2.91	1.43	1.46
6	9.27; 10.70; 11.95	2.92	1.46	1.19
7	9.73; 10.98	2.92	1.92	1.20
8	1.17; 9.99; 10.47	2.89	1.21; 12.40	1.20
9	9.76	3.15	1.20	1.20
10	10.00	3.13	1.44	1.70
11	1.44; 10.00; 11.70	2.91	1.19	1.44
12	10.00	2.91	1.20	1.46

Tab. 10: Numerically and experimentally obtained values of natural frequencies.

j	natural frequencies $f_{(j)}$ [Hz]		
	variant 1	variant 2	experiment
1	1.14	1.14	1.17; 1.19; 1.20; 1.21
2	1.46	1.46	1.44; 1.45; 1.46
3	1.68	1.68	1.67; 1.69; 1.70
4	9.86	9.76	9.73; 9.76; 9.99; 10.00
5	9.86	9.95	9.73; 9.76; 9.99; 10.00
6	10.98	10.96	10.47; 10.95; 10.97; 10.98
7	10.98	10.99	10.47; 10.95; 10.97; 10.98
8	11.96	11.95	11.70; 11.95; 12.14; 12.18
9	11.96	11.98	11.70; 11.95; 12.14; 12.18

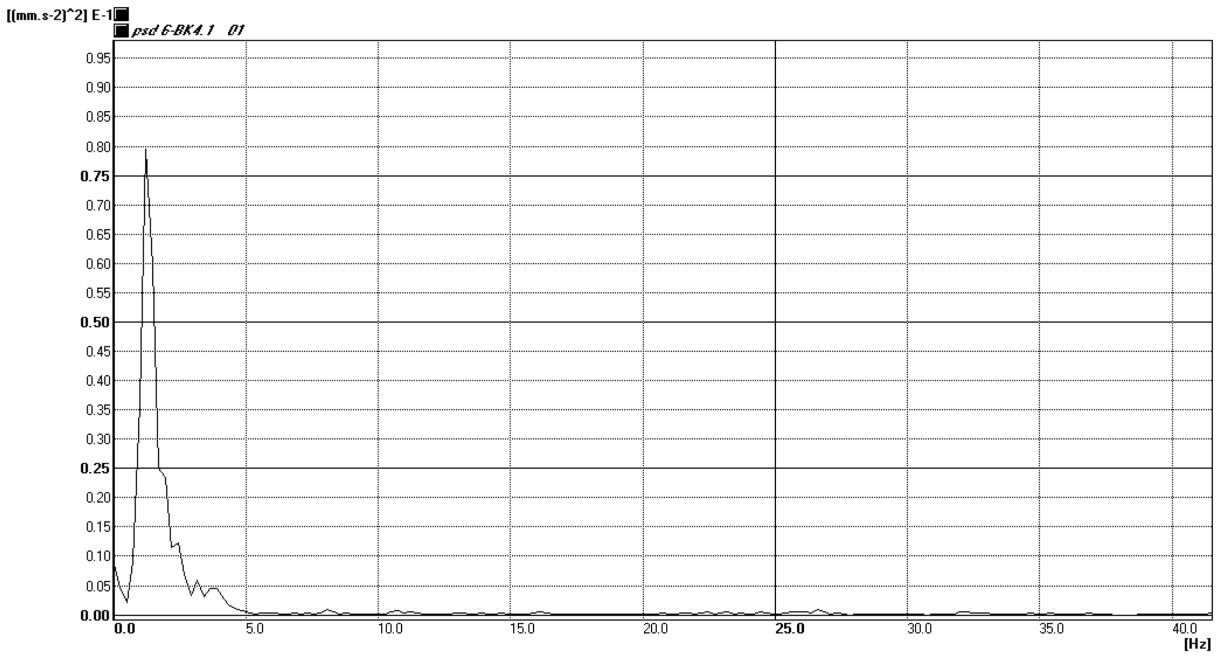

Fig. 3: PSD, run 6, sensor BK4, peak at frequency f = 1.19 Hz.

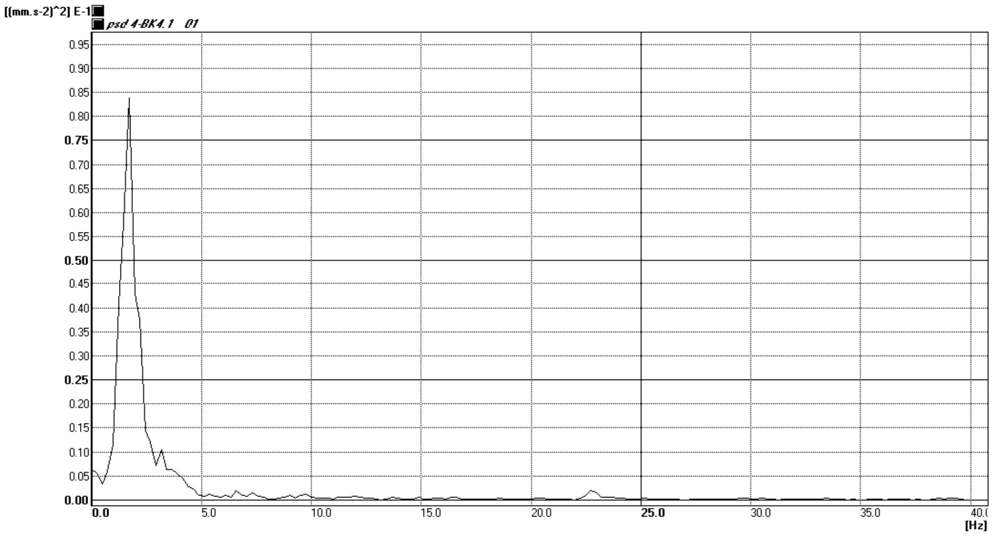

Fig. 4: PSD, run 4, sensor BK4, peak at frequency f = 1.69 Hz.

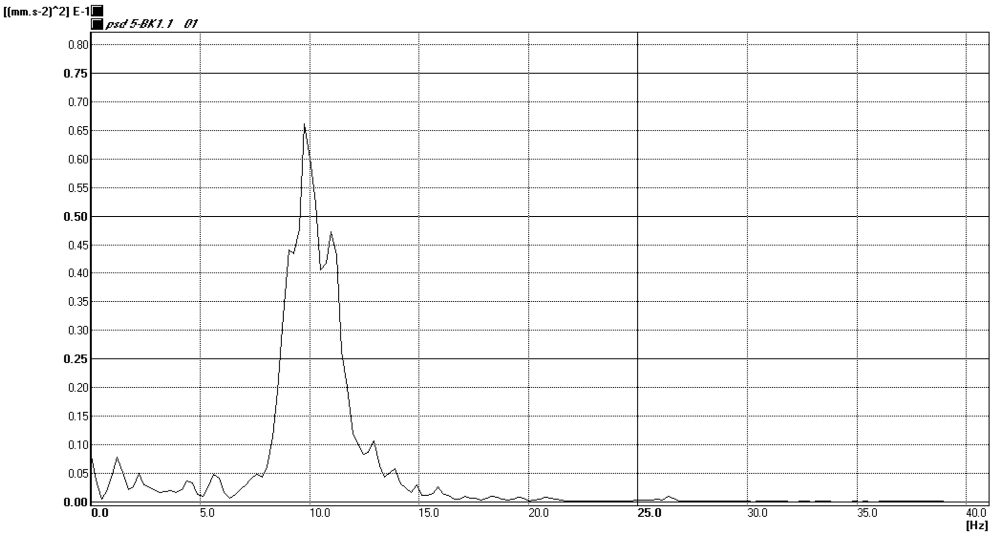

Fig. 5: PSD, run 5, sensor BK4, peak at frequency f = 9.73 and 10.97 Hz.

4 Conclusion

The space computational model of vehicle Tatra 815 was created as multi-body model with 9 degrees of freedom. The modal characteristics of the model were verified by in situ experimental test. The effort was to excite the vibration very closed to natural vibration and to compare experimentally obtained natural frequencies with numerically obtained ones. The results of the test confirm very good agreement between numerically and experimentally obtained values of natural frequencies. Only the frequencies in the range 2.66 – 3.15 Hz are not modeled by vehicle computing model.

Acknowledgement

The work was supported by Grant National Agency VEGA, project No. G1/0005/16.

References

[1] J. Melcer, B. - I. Martinická, Mutual comparison of FRF for various vehicle computational models, Transactions of the VŠB-Technical University of Ostrava 14 (2014) 123–130.